Structure of Hydrogen-Bonded Clusters of 7-Azaindole Studied by IR Dip Spectroscopy and ab Initio Molecular Orbital Calculation

Hiroshi Yokoyama,[†] Hidekazu Watanabe,[‡,§] Takuichiro Omi,[†] Shun-ichi Ishiuchi,[||] and Masaaki Fujii*,[||]

Department of Chemistry, Graduate School of Science and Engineering, Waseda University/PRESTO, Okubo, Shinjuku-ku, Tokyo 169-8555, Japan, RIKEN, The Institute of Physical and Chemical Research, Wako, Saitama, 351-0198, Japan, and Institute for Molecular Science/Graduate School for Advanced Study, Myodaiji, Okazaki 444-8585, Japan

Received: April 3, 2001; In Final Form: July 23, 2001

The IR spectrum of 7-azaindole monomer, 7-azaindole reactive and nonreactive dimers, and (7-azaindole)-$(H_2O)_n$ ($n = 1-3$) clusters in a supersonic jet from 2600 to 3800 cm^{-1} have been measured using IR dip spectroscopy. The vibrational transitions in the ground state were clearly observed and were assigned to the CH and NH stretching vibrations of 7-azaindole and the OH stretching vibrations of water molecules in the clusters. The observed IR spectra of 7-azaindole monomer and (7-azaindole)$(H_2O)_n$ ($n = 1-3$) clusters were compared to theoretical ones obtained by ab initio MO calculations. From a comparison, it is concluded that (7-azaindole)$(H_2O)_n$ ($n = 1-3$) clusters have a ring structure due to a cyclic hydrogen-bond network. This conclusion is consistent with an analysis based on high-resolution spectroscopy. Similarly, the IR dip spectrum suggests that the 7-azaindole reactive dimer has a cyclic hydrogen-bond network, forming a symmetric planar structure. It is strongly suggested from the IR spectrum and the ab initio calculations that the nonreactive dimer contains a water molecule between 7-azaindole molecules.

1. Introduction

7-Azaindole (7-AzI) dimer has been regarded as a model for the hydrogen-bonded base pair of DNA and has been suggested to provide information about a mechanism involving the mutation of DNA pairs.[1−3] From this motivation, 7-AzI dimer and 7-AzI hydrogen-bonded clusters have been studied extensively. As for the dynamics of the excited-state tautomerization of the 7-AzI hydrogen-bonded clusters, both experimental[1−14] and theoretical studies[15−18] have been reported. The detailed electronic structure of 7-AzI dimer was studied by using a supersonic jet, and the mechanism of proton transfer (concerted or stepwise) has been discussed extensively.[13,19−24] Another important point concerning the 7-AzI dimer is the existence of two conformational isomers, which have different reactivities for the proton-transfer reaction (reactive and nonreactive dimers).[25,26] The reactive dimer causes an excited-state proton transfer, even from the zero vibrational level of the S_1 state. The evidence of the proton transfer is its visible fluorescence after UV excitation. On the other hand, the nonreactive dimer causes the emission of only ultraviolet fluorescence, which means no proton-transfer reaction. Despite a large difference in the reactivity, the electronic transitions of both isomers are separated by only 38 cm^{-1}.[25,26] This suggests that the stabilities of both dimers are also close in energy.[27] Also, it has been found that the proton-transfer reaction of the 7-AzI reactive dimer is accelerated by vibrational excitation along the intermolecular symmetric stretching mode.[26] To understand the large difference in the reactivity between isomers, the geometry of the 7-AzI dimers provides indispensable information.

However, the geometric structures of dimers and their relation to the reactivities have not been established. As for the reactive dimer, only theoretical studies have been reported.[16,28] The geometrical structure of the nonreactive dimer has been investigated by high-resolution laser-induced fluorescence spectroscopy.[29] Although a T-shaped structure was proposed on the basis of the rotational contour, as the authors mentioned, the proposed geometry contains some ambiguity. Therefore, further experimental and theoretical studies are necessary for the dimers in order to understand their reactivities.

In contrast to the dimers, the structures of the 7-AzI aqueous clusters have been studied well in both an experiment[29] and theory.[17,18,28,30] The rotational analysis based on high-resolution LIF spectroscopy has determined the geometry of 7-AzI$(H_2O)_n$ ($n = 1-3$) as a cyclic hydrogen-bonded network.[29] The rotational analysis is highly reliable for small clusters such as 7-AzI$(H_2O)_1$; however, the ambiguity still remains in the analysis of a larger cluster like 7-AzI$(H_2O)_3$. Thus, further structural study by an alternative method, such as the vibrtational spectroscopy, should be applied. In addition, it has been reported that proton transfer is accelerated by excitation of the intermolecular stretching vibration in S_1.[26] Thus, vibrations concerning the hydrogen bond, such as NH and OH stretching, should be measured.

In this work, we investigated the geometric structures of the 7-AzI reactive dimer, the nonreactive dimer, and 7-AzI$(H_2O)_n$ ($n = 1-3$) clusters in the ground state by IR spectroscopy. Since the frequency of the NH stretching vibration (ν_{NH}) and the OH

* To whom all correspondence should be addressed. E-mail: mfujii@ims.ac.jp.
[†] Waseda University/PRESTO.
[‡] RIKEN.
[§] Present address: AIST Shikoku, National Institute of Advanced Industrial Science and Technology (AIST), 2217-14 Hayashi-cho, Takamatsu-shi, Kagawa 761-0395, Japan.
[||] Institute for Molecular Science/Graduate School for Advanced Study.

10.1021/jp011245g CCC: $20.00
Published on Web 09/26/2001

stretching vibration (ν_{OH}) reflect the hydrogen-bonding sensitively, structural information can be obtained. The IR spectrum of each cluster has been measured by IR dip spectroscopy from 2600 to 3800 cm^{-1}, where ν_{NH} and ν_{OH} appear. The optimized structures and their theoretical spectra have been obtained for 7-AzI dimers and 7-AzI$(H_2O)_n$ by ab initio MO calculations. The IR dip spectra of 7-AzI$(H_2O)_n$ ($n = 1-3$) clusters have been compared to the theoretical spectra, and the geometric structure in the ground state has been determined. Conformations of the reactive and nonreactive dimers have also been determined on the basis of the IR dip spectra and ab initio MO calculations. The relation between the reactivity and the geometry in dimers is discussed.

2. Method

2.1. Experimental Method. The IR spectra of the 7-AzI monomer, 7-AzI$(H_2O)_n$ ($n = 1-3$) clusters, 7-AzI nonreactive dimer, and 7-AzI reactive dimer were measured by IR dip spectroscopy. This spectroscopy has been applied to various solvated clusters,[31−59] including the related cluster (indole)-$(H_2O)_n$.[55,56] The procedure of the measurement is as follows. The UV laser ν_{UV} was fixed to the origin of the $S_1 \leftarrow S_0$ transition. The fluorescence intensity from the S_1 state was monitored while the IR laser ν_{IR} irradiated the sample in a supersonic jet. Here, the IR laser was scanned in the energy region from 2700 to 3800 cm^{-1}. When ν_{IR} was resonant to a certain vibrational level, the fluorescence intensity decreased because of a loss of population in the ground vibrational level. As a result, the vibrational transition in the ground state was detected as a depletion of the fluorescence intensity. This spectroscopy has an advantage in that the vibrational transition of a specific molecular species can be observed by fixing ν_{UV} to an electronic transition of the species.

The experimental setup for the IR dip spectroscopy is described elsewhere.[31,62] Briefly, the second harmonics (532 nm) and the third harmonics (355 nm) of the Nd^{3+}:YAG lasers (HOYA-Continuum Powerlite 8010, Spectra-Physics Quanta-Ray GCR170, respectively) were used to pump two dye lasers (Lumonics HD-500). To generate the IR laser, the second harmonic (532 nm) of the Nd^{3+}:YAG laser was split into two. The output of the dye laser pumped by the 90% of the second harmonic was differentially mixed with the remainder of the second harmonics in a $LiNbO_3$ crystal (Inrad, IR Autotracker II) and was converted to the tunable IR laser ν_{IR} in the 3 μm region. The typical power of ν_{IR} was 0.1−0.5 mJ. The output of the dye laser pumped by the third harmonic of the YAG laser was frequency-doubled by a nonlinear crystal (KDP, Inrad) and converted to a tunable UV laser ν_{UV}. Both ν_{UV} and ν_{IR} were coaxially introduced into a vacuum chamber (Toyama/Hakuto) and were crossed as a supersonic jet. Here, ν_{UV} was delayed by 50 ns with respect to ν_{IR} by a delayed pulse generator (Stanford Research, DG535). The fluorescence from the sample was collected by a lens and detected by a photomultiplier (Hamamatsu 1P28) through color filters (Toshiba UV-35 and Corning 7-54 for the UV fluorescence; Toshiba L-42 for the visible fluorescence). The signal was integrated by a digital boxcar (EG&E PARC model 4420/4422). The integrated signal was recorded by a personal computer (NEC PC9801) as a function of the IR laser frequency.

To minimize the effect of varying of the experimental condition, such as the laser power, both the signal with $\nu_{UV} + \nu_{IR}$ and that due to ν_{UV} only were observed simultaneously by using an alternative data-acquisition system, which has been fully described elsewhere.[61] The IR dip spectrum was divided by the spectrum due to ν_{UV} only, which was obtained in the same scan by operating ν_{UV} at 20 Hz and ν_{IR} at 10 Hz. Both signals were stored in different memories and were integrated separately by the digital boxcar.

The sample vapor at 373 K was seeded in He gas at 2 atm. The water vapor at 0 °C was also seeded in He gas when the 7-AzI aqueous cluster was studied. The mixture was expanded into the vacuum chamber through a solenoid valve operated at 20 Hz. The sample was purchased from Tokyo Kasei and purified by vacuum sublimation.

2.2. Calculation Method. The geometric structures of hydrated 7-azaindole clusters 7-AzI$(H_2O)_n$ ($n \leq 3$), and (7-AzI)$_2$-$(H_2O)_n$ ($n \leq 2$) were determined by an ab initio molecular-orbital method. The approximation used was the with the frozen-core second-order Möller−Plesset method with the 6-31G basis set (MP2/6-31G) for 7-AzI$(H_2O)_n$ ($n \leq 3$) and density functional theory with Beck's three-parameter hybrid method using the LYP correlation functional with the 6-31G basis set (B3LYP/6-31G)[63] for (7-AzI)$_2(H_2O)_n$ ($n \leq 2$). At every optimized structure, the harmonic frequencies were evaluated in order to confirm the true local minimum and to analyze the experimentally observed IR spectra.

To compare with the observed spectra, a scaling factor was uniformly multiplied by the calculated frequencies. For 7-AzI-$(H_2O)_n$ clusters, the scaling factor (0.9845), which was determined with the NH stretching mode of the 7-AzI molecule, and ν_1 and ν_3 of the water molecules, was used. For the (7-AzI)$_2$-$(H_2O)_n$ cluster, the factor 0.9529, which was determined with the NH stretching mode of the 7-AzI monomer, was used.

The programs used for the optimization and the frequency calculations were GAUSSIAN 92,[64] GAUSSIAN 94,[65] and GAUSSIAN 98.[66] The computation was carried out on a computer system at the computer center of Institute for Molecular Science and our local machines.

3. Results and Discussion

3.1. 7-AzI Monomer. Figure 1 shows the IR dip spectrum of the 7-AzI monomer when the UV laser was fixed to its S_1 origin (3 4634 cm^{-1}).[29] The fluorescence intensity due to $\nu_{IR} + \nu_{UV}$ and that due to ν_{UV} only are shown in Figure 1a,b, respectively. The zero point and the intensity without ν_{IR} are also shown besides the spectra. Here, both spectra were obtained in the same frequency-scan by the alternative data acquisition system (see Experimental Section). The fluorescence intensity due to $\nu_{IR} + \nu_{UV}$ decreases at 3521 cm^{-1} and around 3000 cm^{-1} (Figure 1a). Because the fluorescence dips cannot be seen without ν_{IR} (Figure 1b), the dips clearly correspond to the IR absorption of the 7-AzI monomer. According to the IR spectrum in the gas phase,[67] the dip at 3521 cm^{-1} and those at around 3000 cm^{-1} are assigned to ν_{NH} and ν_{CH}, respectively. The observed vibrational wavenumbers and assignments are listed in Table 1.

As can be seen in Figure 1a, the baseline of the spectrum varies slightly. This was caused by a variation of the laser power and/or the pulsed nozzle condition. This variation can be compensated when the signal due to $\nu_{IR} + \nu_{UV}$ is divided by that due to ν_{UV} only.[61] Figure 1c shows the spectrum obtained by taking the ratio of the fluorescence intensity due to $\nu_{IR} + \nu_{UV}$ to that due to ν_{UV} only. Because the baseline is almost linear, the variation can be well canceled by taking the ratio. In this paper, we will show the IR dip spectra of clusters by taking the ratio.

3.2. 7-AzI$(H_2O)_n$ ($n = 1-3$) Clusters. The IR dip spectra of 7-AzI$(H_2O)_n$ ($n = 1-3$) are shown in parts b−d of Figure 2,

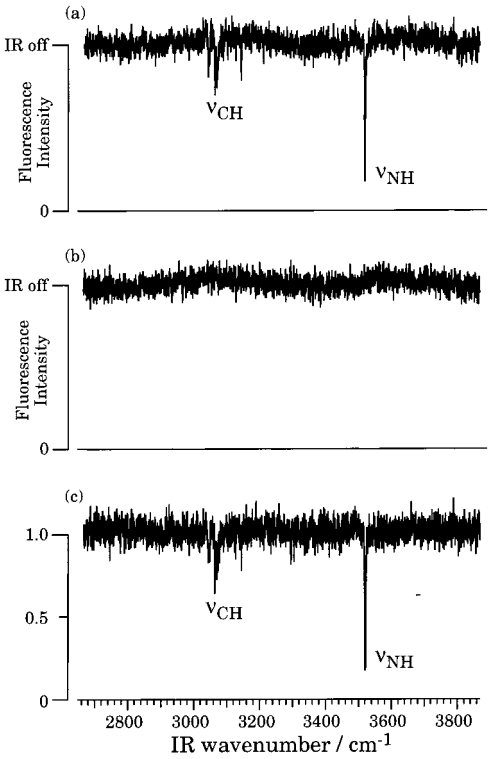

Figure 1. IR dip spectrum of jet-cooled 7-azaindole(7-AzI) monomer (7-AzI). (a) The fluorescence intensity due to $\nu_{IR} + \nu_{UV}$ and (b) that due to ν_{UV} only. (c) IR dip spectrum obtained by taking the ratio of the fluorescence intensity due to $\nu_{IR} + \nu_{UV}$ to that due to ν_{UV} only. A vertical axis shows the ratio.

TABLE 1: Vibrational Assignments of the IR Dip Spectrum of 7-AzI Monomer in a Supersonic Jet

obs freq (cm^{-1})	ref 67	assignment
3049	3042	CH stretch (pyridine ring)
3065	3066	CH stretch (pyridine ring)
3071	3085	CH stretch (pyridine ring)
3104	3100	CH stretch (pyridine ring)
3145	3142.1	CH stretch (pyridine ring)
3521	3517.5	NH stretch

respectively. The frequency of ν_{UV} is fixed to the S_1 origin of each species, which are 33 340, 32 632, and 32 554 cm^{-1} for 7-AzI$(H_2O)_n$ ($n = 1-3$), respectively.[29] The IR dip spectrum of the 7-AzI monomer is also shown in Figure 2a for comparison. The IR dip spectrum of the 7-AzI$(H_2O)_1$ shows an intense band at 3412 cm^{-1} and weak bands at 3369 and 3724 cm^{-1}. From its frequencies, three bands correspond to ν_{NH} and two OH stretching vibrations of the water moiety. Assuming that 7-AzI is a proton donor to the water moiety in the cluster, we assigned the strongest band at 3412 cm^{-1} as ν_{NH} shifted to red by the hydrogen-bond formation. The band at 3724 cm^{-1} is assigned to the non-hydrogen-bonded OH stretch (non-H-bonded OH stretch) of the water moiety, corresponding to the antisymmetric OH stretching ν_3 of a free water. This is because the band is lying in a region higher than ν_{NH} of the 7-AzI monomer (3521 cm^{-1}) and is close to the vibrational frequency of ν_3 of a free water molecule (3756 cm^{-1}).[60] Thus, the rest (3369 cm^{-1}) should be assigned to the hydrogen-bonded OH stretch (H-bonded OH stretch) of the water moiety, corresponding to the OH symmetric stretching ν_1 of a free water. Here, the vibrational modes of non-H-bonded and H-bonded OH stretch are no longer symmetric and antisymmetric stretching modes of a free water molecule, but the vibrations of the cluster. The appearance of a H-bonded OH stretch is clearly different

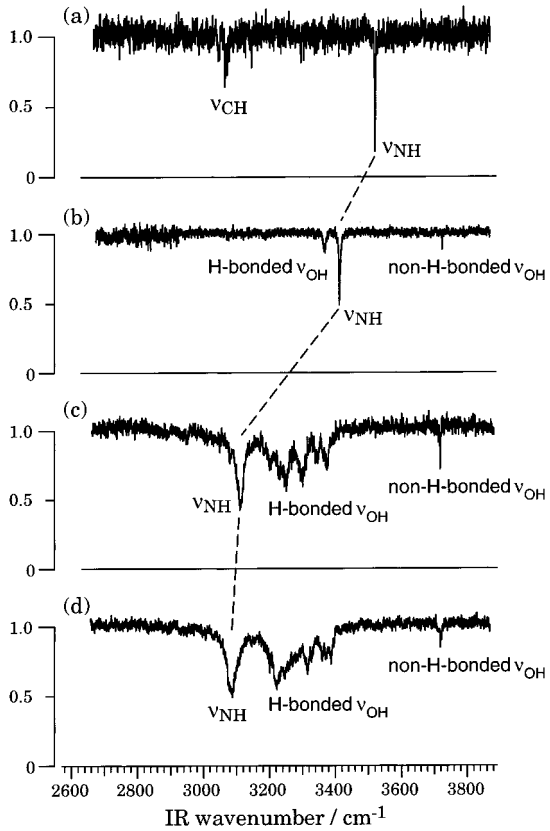

Figure 2. IR dip spectrum of jet-cooled (a) 7-AzI monomer, (b) 7-AzI-$(H_2O)_1$, (c) 7-AzI$(H_2O)_2$, and (d) 7-AzI$(H_2O)_3$. A vertical axis shows the ratio of the fluorescence intensity due to $\nu_{IR} + \nu_{UV}$ to that due to ν_{UV} only.

from the 1:1 aqueous cluster of phenol[33,49] and naphthol.[31,35] In these hydrogen-bonded clusters, a H-bonded OH stretch is absent in the IR spectra. The absence of a H-bonded OH stretch has been explained by the structure of the cluster, where the water molecule is connected to the proton donor by a single hydrogen bond. In this structure, two OH bonds in the water moiety are equivalent as well as a free water molecule in which the symmetric OH stretching has a very weak IR oscillator strength. Therefore, the appearance of a H-bonded OH stretch strongly suggests that the water molecule is asymmetrically bound to 7-AzI through two hydrogen bonds. Further structural information can be obtained from the observed frequency of a H-bonded OH stretch. The frequency 3369 cm^{-1} is significantly shifted to the red from that of a free water molecule (3657 cm^{-1}).[59] This suggests that the water moiety acts not only as a proton acceptor but also as a proton donor in the cluster. We thus conclude that a cyclic hydrogen-bond network is formed in the 7-AzI$(H_2O)_1$ cluster.

Parts c and d of Figure 2 show the IR dip spectrum of 7-AzI-$(H_2O)_2$ and 7-AzI$(H_2O)_3$, respectively. The IR dip spectrum of 7-AzI$(H_2O)_2$ shows an intense broad band at 3112 cm^{-1}, while that of 7-AzI$(H_2O)_3$ shows a strong broad band at 3086 cm^{-1}. We tentatively assign both bands as ν_{NH} of 7-AzI in the cluster, while assuming that 7-AzI is a proton donor. Broadening and a larger red shift of ν_{NH} suggest the stronger hydrogen bond in the larger cluster. The band at 3718 cm^{-1} for each cluster is assigned to a non-H-bonded OH stretch of the water moiety, because of its frequency being higher than ν_{NH} of the monomer. The remaining bands should be assigned to a H-bonded OH stretch of the water moiety. As well as 7-AzI$(H_2O)_1$, the appearance of H-bonded OH stretch bands suggests that water

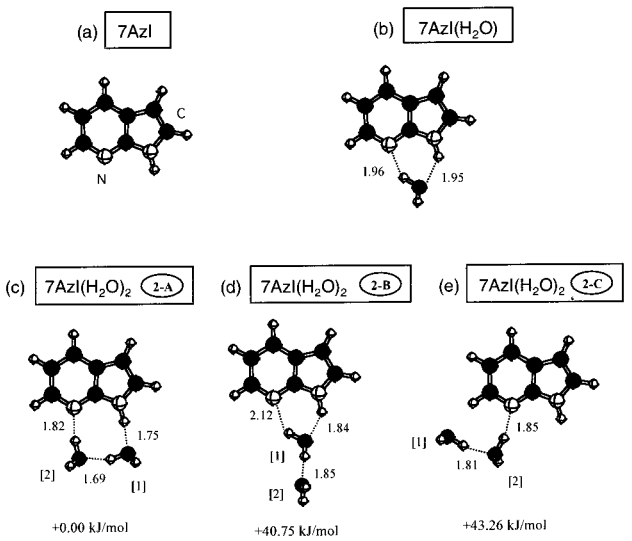

Figure 3. Fully optimized geometries of the (a) bare 7-azaindole (7-AzI) monomer, (b) cluster of 7-azaindole 7-AzI$(H_2O)_1$, and (c)−(e) three isomers of the 7-AzI$(H_2O)_2$ clusters. The optimization is carried out with the MP2/6-31G level. The unit of bond length is given in angstroms. For 7-AzI$(H_2O)_2$, the values under the structures show the relative energy difference given in kJ/mol among the isomers.

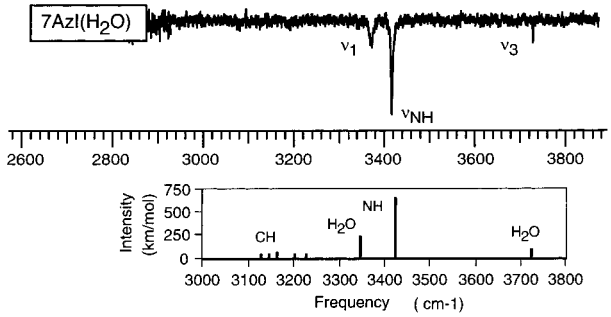

Figure 4. Calculated IR spectrum of the 7-AzI$(H_2O)_1$ clusters evaluated with the MP2/6-31G approximation. The observed IR spectrum is also shown for comparison. The scaling factor 0.9845 is uniformly multiplied to the calculated frequencies.

molecules are asymmetrically bound in the clusters. The structures of the clusters are discussed later on the basis of a comparison with ab initio MO calculations.

3.3. Assignment of the Bands and Structures of 7-AzI Aqueous Clusters on the Basis of ab Initio MO Calculations. *3.3.1. 7-AzI Monomer and 7-AzI$(H_2O)_1$.* The calculated geometries of the monomer and 7-AzI$(H_2O)_n$ ($n = 1-3$) have been reported previously along with a lower level approximation (SCF/6-31G).[29] In this work, we employed a higher approximation (MP2/6-31G) to obtain reliable vibrational frequencies. The optimized geometries of the 7-AzI monomer and 7-AzI$(H_2O)_1$ under the MP2/6-31G level are shown in Figure 3a,b. For 7-AzI$(H_2O)_1$, only the most stable isomer has been calculated (see refs 16, 29, 30, 68, and 69). The 7-AzI molecule plays the role of a proton donor with its NH group and simultaneously acts as a proton acceptor with its N group for the water molecule. The calculated IR spectrum for 7-AzI$(H_2O)_1$ is shown in Figure 4 together with the observed spectrum. The numerical data of the observed and the calculated frequencies are summarized in Table 2. There are three clear bands in the experimental spectrum; the assignments of three bands have already been discussed in the previous section. On the basis of the assignments, a scaling factor (0.9845) was obtained from the average of the ratio of the observed frequency to the calculated one.

TABLE 2: Observed Frequencies (cm^{-1}), Calculated Frequencies (cm^{-1}), and Calculated IR Intensities (km/mol) of NH and OH Stretching Mode for 7-AzI$(H_2O)_n$ ($n = 1-3$) Clusters[a]

		7-AzI NH stretching		H-bonded OH stretching		non-H-bonded OH strething	
		freq	IR intn	freq	IR intn	freq	IR intn
7-AzI$(H_2O)_1$	exp	3412		3369		3724	
	calcd	3428	207.8	3350	633.1	3728	64.2
7-AzI$(H_2O)_2$	exp	3112		3200		3718	
				3251			
				3301			
				3343			
				3374			
	calcd **2-A**	3181	2147.4	3105	20.2	3734	45.6
				3264	585.1	3737	78.0
	calcd **2-B**	3298	659.3	3476	44.4	3610	698.9
				3630	0.0	3795	57.6
	calcd **2-C**	3251	90.1	3251	1034.1	3715	66.1
				3393	350.7	3717	61.5
7-AzI$(H_2O)_3$	exp	3086		3220		3718	
				3316			
				3371			
	calcd **3-A**	3113	3222.9	3047	23.9	3737	72.8
				3176	995.0	3741	46.1
				3242	447.3	3753	57.1
	calcd **3-B**	3322	1578.9	2894	581.2	3572	377.5
				3301	75.7	3721	42.4
				3505	162.3	3760	72.1
	calcd **3-C**	3143	563.6	3044	956.2	3720	55.1
				3159	1045.3	3730	56.2
				3522	379.8	3749	79.2
	calcd **3-D**	3165	20.5	3027	612.3	3576	747.8
				3357	754.2	3727	32.5
				3630	0.3	3794	57.4

[a] The calculated frequencies are evaluated with the MP2/6-31G level, and are scaled with the factor 0.9845, which is determined with ν_{NH} of 7-AzI molecule and ν_1, ν_3 of water molecule of 7-AzI$(H_2O)_1$.

Five CH stretching modes of the 7-AzI moiety are also scaled with the same factor.

3.3.2. 7-AzI$(H_2O)_2$. Parts c−e of Figure 3 show the optimized geometries of 7-AzI$(H_2O)_2$. Three isomers are shown for 7-AzI$(H_2O)_2$ in the figure. The most stable isomer of 7-AzI$(H_2O)_2$ is **2-A**, which has a single ring structure constructed with hydrogen bonds. Two other isomers, **2-B** and **2-C**, are much less stable than isomer **2-A**, and the values under their structures in the figure are the relative energy differences given in kJ/mol with the MP2/6-31G level.

The calculated stick IR spectra of 7-AzI$(H_2O)_2$ are shown in Figure 5 together with the observed spectra for a comparison. The identification for the water moiety ([1] and [2]) corresponds to the structures shown in Figure 3c−e. Table 2 gives the numerical data of the observed and the calculated frequencies. There is no band in the region between 3400 and 3700 cm^{-1} of the observed spectra, and the absence of a vibrational band is well reproduced in the calculated IR spectra of isomer **2-A**. In two other isomers, the calculated IR spectra have several bands in this region. Therefore, it is concluded that 7-AzI$(H_2O)_2$ has the single cyclic geometry shown in **2-A**.

From a comparison with the calculated spectrum for **2-A**, the strong band at 3112 cm^{-1} in the observed spectrum can be assigned to the NH stretching vibration of the 7-AzI moiety, and the small band at 3718 cm^{-1} is the non-H-bonded OH stretching vibration of the water moiety. In the region between 3200 and 3400 cm^{-1}, more than five vibrational bands are observed. However, a possible vibration in this region is the H-bonded OH stretching vibration of a water molecule [1] in the cluster; the H-bonded OH stretching due to another water

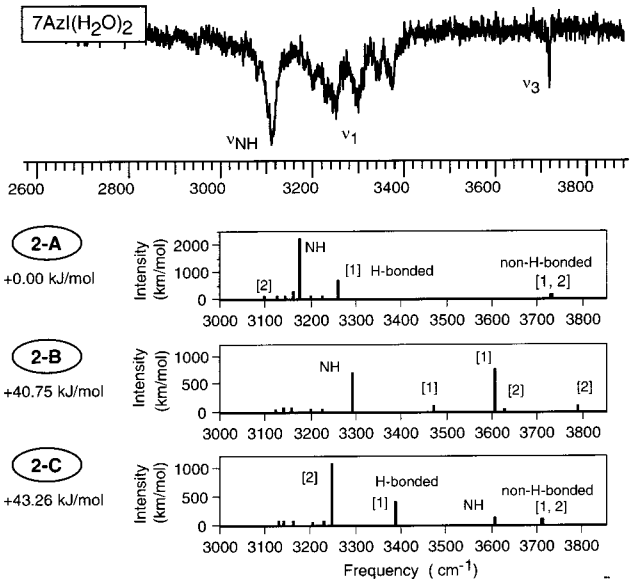

Figure 5. Calculated IR spectra of three isomers of 7-AzI$(H_2O)_2$ clusters evaluated with the MP2/6-31G approximation. The observed IR spectrum is also shown for comparison. The scaling factor 0.9845 is uniformly multiplied to the calculated frequencies.

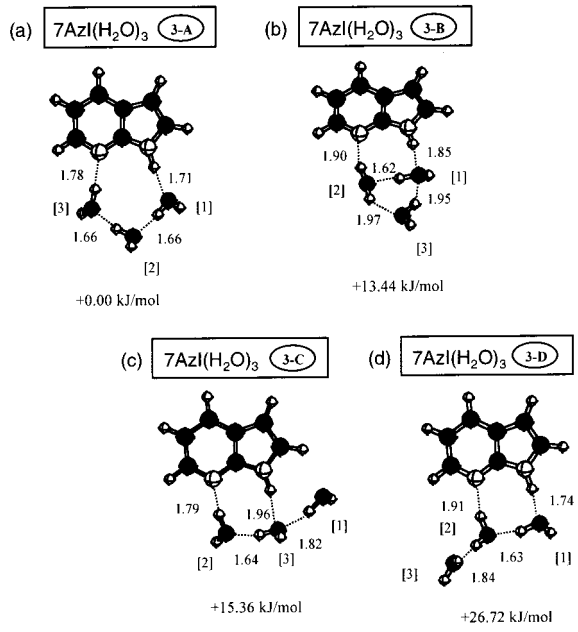

Figure 6. Fully optimized geometries of the 7-AzI$(H_2O)_3$ clusters determined with the MP2/6-31G level. The values under the structures show the relative energy difference given in kJ/mol among the isomers.

molecule [2] was calculated to be 3105 cm^{-1}. Therefore, five vibrations in this region must be considered to be overtones and the combination bands of low-frequency modes.

3.3.3. 7-AzI(H2O)3. Four isomers are shown for 7-AzI$(H_2O)_3$ in Figure 6a−d. Isomer **3-A** is a single ring structure, and isomer **3-B** has a structure in which the 7-AzI molecule and the cyclic water trimer $(H_2O)_3$ are associated. Isomers **3-C** and **3-D** have a structure in which one water molecule is externally bonded to isomer **2-A** of the 7-AzI$(H_2O)_2$ cluster. The most stable isomer is **3-A**. The calculated IR spectra of 7-AzI$(H_2O)_3$ are shown in Figure 7. Numerical data are summarized in Table 3. For isomer **3-A**, the frequency region of the H-bonded OH stretching vibrations of water molecules and ν_{NH} of 7-AzI

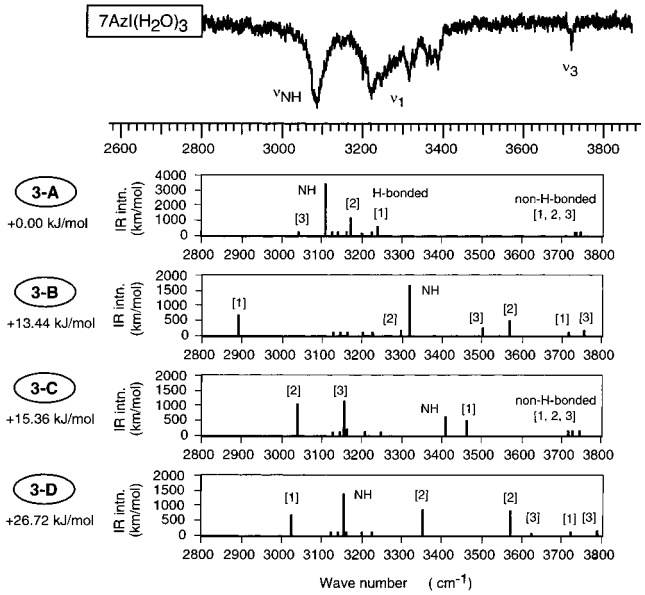

Figure 7. Calculated IR spectra of four isomers of 7-AzI$(H_2O)_3$ clusters evaluated with the MP2/6-31G approximation. The observed IR spectrum is also shown for comparison. The scaling factor 0.9845 is uniformly multiplied to the calculated freqencies.

TABLE 3: Calculated Frequencies (cm^{-1}) and IR Intensities (km/mol) of NH and OH Stretching Mode (cm^{-1}) for (7-AzI)$_2$(H$_2$O)$_n$ (n = 0−2) Clusters

		7-AzI NH stretching		H-bonded OH stretching		non-H-bonded OH strething	
		freq	IR intn	freq	IR intn	freq	IR intn
$(7\text{-AzI})_2$	dimer A	2965	0.0				
		3012	4016.8				
	dimer B	3111	1786.8				
		3523	58.5				
	dimer C	3522	0.0				
		3522	122.3				
	dimer D	3448	436.3				
		3519	71.5				
$(7\text{-AzI})_2(H_2O)_1$	A	2097	975.0	2700	2310.6	3575	33.8
		3022	2346.5				
	B	2963	351.0	3433	64.7	3595	58.8
		3019	3667.0				
$(7\text{-AzI})_2(H_2O)_2$	A	3086	3154.0	2248	2089.3	3303	351.2
		3045	214.3	3091	1516.7	3565	30.0
	B	2934	2205.8	2670	930.1	3167	350.4
		3252	841.3	2845	2470.5	3596	37.4

The calculated frequencies are evaluated with the MP2/6-31G level, and are scaled with the factor 0.9529, which is determined with ν_{NH} of 7-AzI monomer.

molecule are largely shifted to the red and almost overlap with the CH stretching modes of the 7-AzI molecule.

The observed IR spectrum of 7-AzI$(H_2O)_3$ has an interval region where no vibrational band appears (from 3400 to 3700 cm^{-1}). This interval region can be reproduced by isomer **3-A**. On the other hand, in the calculated IR spectra of three other isomers, there exists several bands between 3500 and 3600 cm^{-1}, and the observed spectrum cannot be identified with the spectra of isomers **3-B**, **3-C**, and **3-D**. Furthermore, ν_{NH} in the calculated spectrum of **3-A** matches the observed one in both frequency and relative intensity. Therefore, it is concluded that the geometry of 7AzI$(H_2O)_3$ is **3-A**.

In the calculated spectrum of **3-A**, there are two bands of the H-bonded OH stretching vibrations in the higher frequency region of the NH stretching vibration. However, the observed spectrum shows more than 2 vibrational bands in the region 3300−3400 cm^{-1}. Hence, the existence of the overtones and

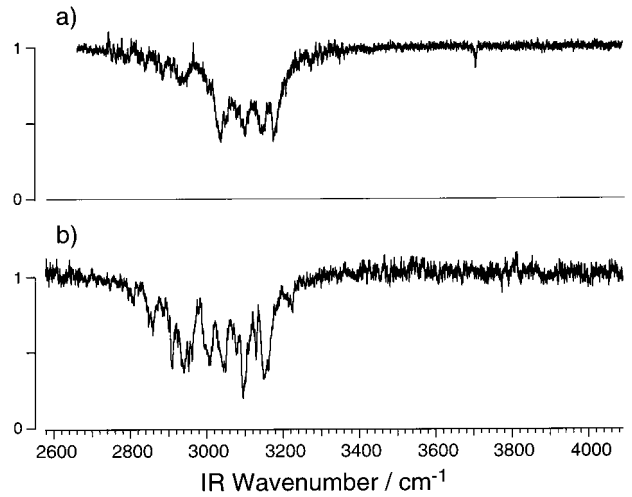

Figure 8. IR dip spectrum of (a) 7-azaindole reactive dimer and (b) nonreactive dimer. A vertical axis shows the ratio of the fluorescence intensity due to $\nu_{IR} + \nu_{UV}$ to that due to ν_{UV} only.

combination bands is considerable in the spectrum of 7-AzI-$(H_2O)_3$ as well as in that of 7-AzI$(H_2O)_2$.

In summary, the most stable isomer of 7-AzI$(H_2O)_n$ up to $n = 3$ is the single ring structure constructed through hydrogen bonds. The present results are consistent with a previous study of the rotationally resolved laser-induced fluorescence spectra by Nakajima et al.,[29] and the cyclic hydrogen-bonded structure is confirmed. The single ring structure is also found in the related cluster (indole)$(H_2O)_n$, in which the water molecules form a bridge from NH to the π ring.[55,56] The different termination of the bridge suggests the difference of the proton affinity between the π electron cloud (indole) and nonbonding electron at N atom (7-azaindole).

3.4. 7-AzI Dimer. Figure 8 shows the IR dip spectra of 7-AzI dimers. The IR spectrum of the proton-transfer reactive dimer is shown in Figure 8a, while that of the nonreactive dimer is presented in Figure 8b. Although the reactive dimer shows a complicated vibrational structure around 3000 cm^{-1}, no band has been found in the region higher than 3200 cm^{-1}. The absence of a band above 3200 cm^{-1} strongly suggests that two NH bonds in the dimer are bonded by hydrogen bonding. This means that the reactive dimer has a ring structure. The complicated structure may originate from CH stretching vibrations, which are enhanced by a Fermi resonance with NH stretching.

The IR spectrum of a nonreactive dimer also shows a complicated vibrational structure at around 3000 cm^{-1} (Figure 8b). However, nonreactive species shows a vibrational band at 3706 cm^{-1} in addition to the cluster of bands at ~3000 cm^{-1}. It is hard to assign this band to a NH stretching vibration in the dimer, because the NH stretching vibration in 7-AzI monomer is 3521 cm^{-1}. The hydrogen-bond formation usually makes the vibrational frequency lower. From its frequency, it is strongly suggested that this band is a non-H-bonded OH stretching vibration and that the nonreactive "dimer" contains water molecules in the cluster. The assignments are discussed on the basis of an ab initio MO calculation in the next section.

3.5. Assignment of the Bands and Structures of 7-AzI Dimer on the Basis of ab Initio MO Calculations. Figure 9 shows optimized structures of $(7\text{-AzI})_2$ obtained with the B3LYP/6-31G level. Four isomers are shown with a relative energy difference in kJ/mol. Here, dimers A, B, and C have a planar structures, while dimer D is nonplanar. The most stable isomer is dimer A, which is a well-investigated ring structure.[17,26] The three other isomers are much less stable than dimer A. Dimer B has only one hydrogen bond between the NH group of 7-AzI [A] and the N atom of 7-AzI [B]. There is no such hydrogen bond in dimer C. We have tried to find a T-shape structure in which two 7-AzI molecules are associated with π-hydrogen bonds. Although the dimer of the T-shape is often considered to be a nonreactive dimer, it has not been found. Instead, we have found dimer D, whose geometry becomes largely broken from a T-shape structure (see also views from other two angles).

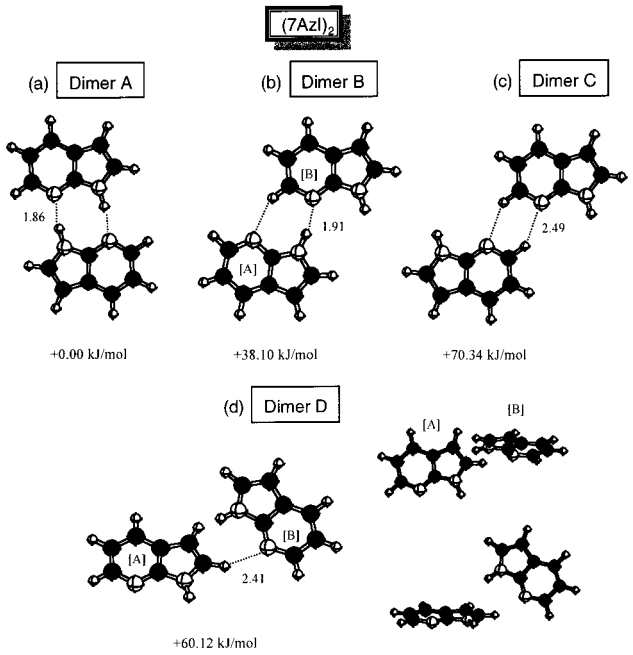

Figure 9. Fully optimized geometries of four isomers of 7-azaindole dimers. The optimization is carried out with the B3LYP/6-31G level. For isomer (d), views from other two angles are also shown. The unit of bond length is given in angstroms. The values under the structures show the relative energy difference given in kJ/mol among the isomers.

The calculated the IR spectra of dimers A, B, C, and D are shown in Figure 10. The observed IR dip spectrum of the reactive dimer is also shown in the figure. The numerical data of the frequencies are summarized in Table 3. The characteristic feature of the observed IR spectrum is the absence of vibrations in the region above 3200 cm^{-1}. This interval region is well reproduced in the calculated spectrum of dimer A, in which both NH bonds are bound by hydrogen bonding. Three other isomers have free NH group(s), and their frequencies of stretching vibration are close to 3521 cm^{-1}, which is the NH stretching vibration of the monomer 7-AzI molecule. It is concluded that the reactive dimer can be identified as dimer A of the ring structure with the spectroscopic technique for the first time.

Figure 11 shows the optimized structures of $(7\text{-AzI})_2(H_2O)$ and $(7\text{-AzI})_2(H_2O)_2$ together with a view from another angle. Two isomers are shown for each size of the clusters. The values under the structures are the relative energy difference between the isomers. The most stable structure of $(7\text{-AzI})_2(H_2O)$ is isomer A, in which the water molecule is inserted into two 7-AzI molecules. By inserting a water molecule, the structure of isomer A becomes nonplanar. However, in isomer B, the water molecule is over the 7-AzI molecule with π-hydrogen bonding, and the cyclic planar structure of 7-AzI dimer core is held.

The most stable isomer of $(7\text{-AzI})_2(H_2O)_2$ is isomer A of the insertion structure. Two water molecules, [1] and [2], also make hydrogen-bonding. The structure of this isomer also becomes nonplanar because of the insertion of water molecules. Isomer

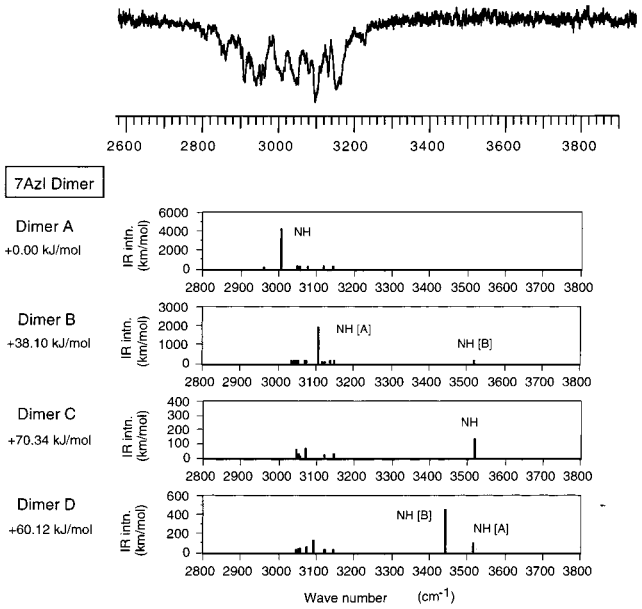

Figure 10. Calculated IR spectra of four isomers of 7-azaindole dimers evaluated with the B3LYP/6-31G level together with the observed IR spectum for the reactive dimer. The scaling factor 0.9529 is uniformly multiplied to the calculated frequencies.

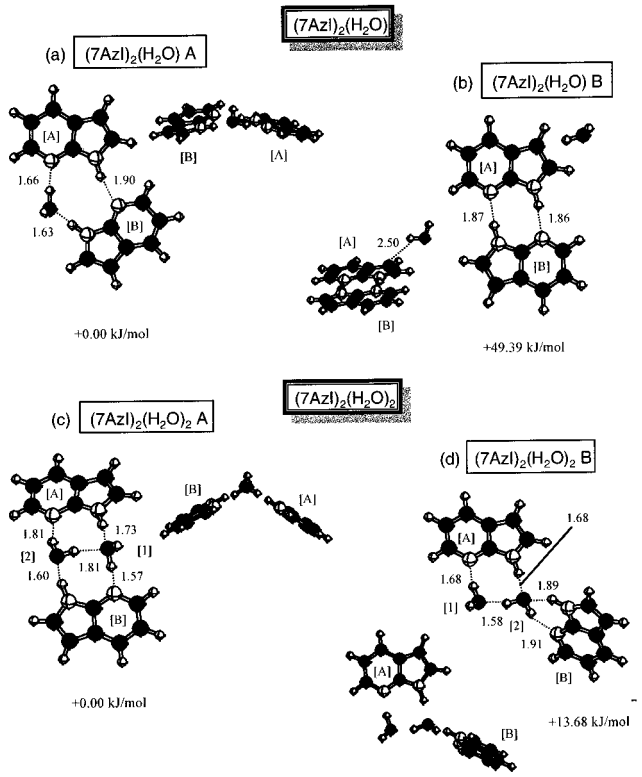

Figure 11. Fully optimized geometries of (a, b) $(7\text{-AzI})_2(H_2O)_1$ clusters and (c, d) $(7\text{-AzI})_2(H_2O)_2$ clusters. The optimization is carried out with the B3LYP/6-31G level. A view from another angle is also shown for each structure. The unit of bond length is given in angstroms. The values under the structures show the relative energy difference given in kJ/mol among the isomers.

B of $(7\text{-AzI})_2(H_2O)_2$ has a double ring structure. 7-AzI [A], water [1], and water [2] make the substructure just like $(7\text{-AzI})(H_2O)_2$ (**2-A**), and 7-AzI [B] and water [2] make the substructure like $(7\text{-AzI})(H_2O)$.

The calculated IR spectra of $(7\text{-AzI})(H_2O)_1$ and $(7\text{-AzI})(H_2O)_2$ together with the observed IR dip spectrum of the nonreactive dimer are shown in Figure 12. All of calculated spectra have a band of a non-H-bonded OH stretching vibration at around 3600 cm^{-1}. It corresponds to the characteristic band at 3706 cm^{-1} in the observed IR spectrum of a nonreactive dimer. Another characteristic feature of the observed IR spectrum is the absence of a band from 3200 to 3700 cm^{-1}. This interval region is reproduced by the calculated spectrum of isomer A of $(7\text{-AzI})_2(H_2O)_1$. All other isomers show vibrations in this interval region, as can be seen in the figure. Therefore, we have concluded that the nonreactive dimer contains a water molecule with two 7-AzI molecules and has the water-inserted ring structure of $(7\text{-AzI})_2(H_2O)_1$ (isomer A).

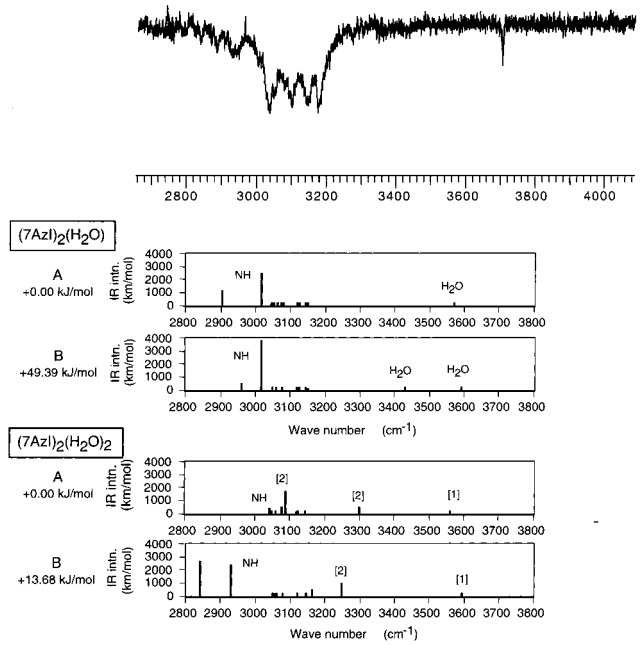

Figure 12. Calculated IR spectra of $(7\text{-AzI})_2(H_2O)_1$ and $(7\text{-AzI})_2(H_2O)_2$ clusters evaluated with the B3LYP/6-31G level together with the observed IR spectum for the nonreactive dimer. The scaling factor 0.9529 is uniformly multiplied to the calculated frequencies.

3.6. Discussion. Let us discuss the consistency of the obtained structures with the previously reported photochemical property of reactive and nonreactive dimers. Since the cyclic geometry of the reactive dimer was strongly suggested previously, it will be no problem to understand its reactivity in a double proton transfer when it is excited to the S_1 state. The low reactivity of a nonreactive dimer can be naturally understood from its structure. Because of the insertion of a water molecule in the hydrogen-bonded ring, the N−H···N bonds deviate from linear. Because this nonlinear configuration is not feasible for hydrogen bonding, proton transfer in the dimer is prevented. In addition, the asymmetry due to the presence of the water molecule affects the potential curve and the double proton transfer might be suppressed much.

The second characteristic point of the nonreactive dimer is that its stability is considered to be comparable to the reactive dimer. The water-inserted ring structure is also reasonable for a large stability in energy. In the water-inserted cyclic dimer, the N−H···N hydrogen bond has lower stabilization than that in the reactive dimer, because of its nonlinear configuration. However, it has a total of three hydrogen bonds among two 7-AzI and water molecules. Therefore, the total stabilization energy is expected to be comparable to the pure, reactive 7-AzI dimer.

The last point is the mass spectrum obtained via a S_1-S_0 transition of a nonreactive dimer. Though we have concluded

the water-inserted ring structure for the nonreactive dimer, the observed mass number just coincides with that of the pure dimer $(7\text{-AzI})_2$ ($m/z = 236$). This means that the water molecule in the aqueous dimer must be evaporated after ionization. The perfect evaporation of the water moiety has also been found in the $(\text{indole})(H_2O)_2$ cluster;[56,57] therefore it is a probable assumption. For the nonreactive 7-AzI dimer, the perfect evaporation may be related to the structure of the 7-AzI dimer cation. Many aromatic dimer cations show large stabilization by forming a charge resonance structure. In the charge resonance dimer, two molecules locate at an equivalent position, and the largest stabilization is obtained when π orbitals overlap largely, such as a parallel sandwich structure.[70,71] Then, it is natural that the most stable structure of the 7-AzI dimer becomes a parallel sandwich structure after ionization. If so, the vertical ionization from the water-inserted cyclic dimer would cause a large vibrational excitation along the intermolecular coordinate and the water molecule would be dissociated immediately.

In conclusion, the geometry of $7\text{-AzI}(H_2O)_n$ ($n = 1-3$) and reactive and nonreactive 7-AzI dimers are determined by the combination of the IR dip spectrum and the ab initio MO calculations. The ring structure of the reactive dimer was experimentally determined for the first time. It is revealed that the nonreactive dimer is not the pure dimer of 7-AzI but is an aqueous dimer, i.e., $(7\text{-AzI})_2(H_2O)_n$. On the basis of a comparison between the observed and calculated spectra for various candidates, it is concluded that nonreactive dimer has a water-inserted ring structure of $(7\text{-AzI})_2(H_2O)_1$.

Acknowledgment. The research was financially supported in part by Grants-in-Aid from the Ministry of Education, Science, Sports, and Culture, Japan, and The Daiko Foundation. H.W. gives thanks for the financial support of Special Postdoctoral Researchers Program in RIKEN.

References and Notes

(1) Taylor, C. A.; El-Bayoumi, M. A.; Kasha, M. *Proc. Natl. Acad. Sci. U.S.A.* **1969**, *63*, 253.
(2) Ingham, K. C.; Elgheit, M. A.; El-Bayoumi, M. A. *J. Am. Chem. Soc.* **1971**, *93*, 5023.
(3) Ingham, K. C.; El-Bayoumi, M. A. *J. Am. Chem. Soc.* **1974**, *96*, 1674.
(4) El-Bayoumi, M. A.; Avouris, P.; Ware, W. R. *J. Chem. Phys.* **1975**, *62*, 2499.
(5) Avouris, P.; Yang, L. L.; El-Bayoumi, M. A. *Photochem. Photobiol.* **1976**, *24*, 211.
(6) McMorrow, D.; Aartsma, T. J. *Chem. Phys. Lett.* **1986**, *125*, 581.
(7) Tokumura, K.; Watanabe, Y.; Udagawa, M.; Itoh, M. *J. Am. Chem. Soc.* **1987**, *109*, 1346.
(8) Chou, P. T.; Martinez, M. L.; Cooper, W. C.; McMorrow, D.; Collins, S. T.; Kasha, M. *J. Phys. Chem.* **1992**, *96*, 5203.
(9) Douhal, A.; Kim, S. K.; Zewail, A. H. *Nature* **1995**, *378*, 260.
(10) Chachisvilis, M.; Fiebig, T.; Douhal, A.; Zewail, A. H. *J. Phys. Chem.* **1998**, *A102*, 669.
(11) Suzuki, T.; Okuyama, U.; Ichimura, T. *J. Phys. Chem.* **1997**, *A101*, 7047.
(12) Takeuchi, S.; Tahara, T. *Chem. Phys. Lett.* **1997**, *277*, 340.
(13) Takeuchi, S.; Tahara, T. *J. Phys. Chem.* **1998**, *A102*, 7740.
(14) Smirnov, A. V.; English, D. S.; Rich, R. L.; Lane, J.; Teyton, L.; Schwabacher, A. W.; Luo, S.; Thornburg, R. W.; Petrich, J. W. *J. Phys. Chem.* **1997**, *B101*, 2758.
(15) Waluk, J.; Bulska, H.; Grabowska, A.; Mordzinski, A. *New J. Chem.* **1986**, *10*, 413.
(16) Douhal, A.; Guallar, V.: Moreno, M.; Lluch, J. M. *Chem. Phys. Lett.* **1996**, *256*, 370.
(17) Shukla, M. K.; Mishra, P. C. *Chem. Phys.* **1998**, *230*, 187.
(18) Chaban, G. M.; Gordon, M. S. *J. Phys. Chem.* **1999**, *A103*, 185.
(19) Douhal, A.; Moreno, M.; Lluch, J. M. *Chem. Phys. Lett.* **2000**, *324*, 75.
(20) Douhal, A.; Moreno, M.; Lluch, J. M. *Chem. Phys. Lett.* **2000**, *324*, 81.
(21) Folmer, D. E.; Poth, L.; Wisniewski, E. S.; Castleman, A. W., Jr. *Chem. Phys. Lett.* **1998**, *287*, 1.
(22) Folmer, D. E.; Wisniewski, E. S.; Castleman Jr., A. W. *Chem. Phys. Lett.* **2000**, *318*, 637.
(23) Catalán, J.; del Valle, J. C.; Kasha, M. *Proc. Natl. Acad. Sci.* **1999**, *96*, 8338.
(24) Catalán, J.; del Valle, J. C.; Kasha, M. *Chem. Phys. Lett.* **2000**, *318*, 629.
(25) Fuke, K.; Yoshiuchi, H.; Kaya, K. *J. Phys. Chem.* **1984**, *88*, 5840.
(26) Fuke, K.; Kaya, K. *J. Phys. Chem.* **1989**, *93*, 614.
(27) Abe, H.; Mikami, N.; Ito, M. *J. Phys. Chem.* **1982**, *86*, 1768.
(28) Chou, P. T.; Wei, C. Y.; Chang, C. P.; Meng-Shin, K. *J. Phys. Chem.* **1995**, *99*, 11994.
(29) Nakajima, A.; Hirano, M.; Hasumi, R.; Kaya, K.; Watanabe, H.; Carter, C. C.; Williamson, J. M.; Miller, T. A. *J. Phys. Chem.* **1997**, *A101*, 392.
(30) Kim, S. K.; Bernstein, E. R. *J. Phys. Chem.* **1990**, *94*, 3531.
(31) Yoshino, R.; Hashimoto, K.; Omi, T.; Ishiuchi, S.; Fujii, M. *J. Phys. Chem.* **1998**, *A102*, 6227.
(32) Ishiuchi, S.; Saeki, M.; Sakai, M.; Fujii, M. *Chem. Phys. Lett.* **2000**, *322*, 27.
(33) Tanabe, S.; Ebata, T.; Fujii, M.; Mikami, N. *Chem. Phys. Lett.* **1993**, *215*, 347.
(34) Watanabe, T.; Ebata, T.; Tanabe, S.; Mikami, N. *J. Chem. Phys.* **1996**, *105*, 408.
(35) Matsumto, Y.; Ebata, T.; Mikami, N. *J. Chem. Phys.* **1998**, *109*, 6303.
(36) Iwasaki, A.; Fujii, A.; Watanabe, T.; Ebata, T.; Mikami, N. *J. Phys. Chem.* **1996**, *100*, 16053.
(37) Matsumoto, Y.; Ebata, T.; Mikami, N. *J. Chem. Phys.* **1998**, *109*, 6303.
(38) Guchhait, N.; Ebata, T.; Mikami, N. *J. Chem. Phys.* **1999**, *111*, 8438.
(39) Matsumoto, Y.; Ebata, T.; Mikami, N. *J. Mol. Struct.* **2000**, *552*, 257.
(40) Ebata, T.; Fujii, A.; Mikami, N. *Int. Rev. Phys. Chem.* **1998**, *17*, 331 and reference therein.
(41) Riehn, C.; Lahmann, C.; Wassermann, B.; Brutschy, B. *Chem. Phys. Lett.* **1992**, *197*, 443.
(42) Tarakeshwar, P.; Kim., K. S.; Brutschy, B. *J. Chem. Phys.* **1999**, *110*, 8501; **2000**, *112*, 1769.
(43) Buchhold, K.; Reimann, B.; Djafari, S.; Barth, H. D.; Brutschy, B.; Tarakeshwar, P.; Kim, K. S. *J. Chem. Phys.* **2000**, *112*, 1844.
(44) Riehn, C.; Buchhold, K.; Reimann, B.; Djafari, S.; Barth, H. D.; Brutschy, B.; Tarakeshwar, P.; Kim, K. S. *J. Chem. Phys.* **2000**, *112*, 1170.
(45) Brutschy, B. *Chem. Rev.* **2000**, *100*, 3891 and references therein.
(46) Gerhards, M.; Unterberg, C.; Kleinermanns, K. *Phys. Chem. Chem. Phys.* **2000**, *2*, 5538.
(47) Schmitt, M.; Jacoby, C.; Gerhards, M.; Unterberg, C.; Roth, W.; Kleinermanns, K. *J. Chem. Phys.* **2000**, *113*, 2995.
(48) Spangenberg, D.; Imhof, P.; Roth, W.; Janzen, C.; Kleinermanns, K. *J. Phys. Chem.* **1999**, *A103*, 5918.
(49) Kleinermanns, K.; Janzen, C.; Spangenberg, D.; Gerhards, M. *J. Phys. Chem.* **1999**, *A103*, 5232.
(50) Janzen, C.; Spangenberg, D.; Roth, W.; Kleinermanns, K. *J. Chem. Phys.* **1999**, *110*, 9898.
(51) Jacoby, C.; Roth, W.; Schmitt, M.; Janzen, C.; Spangenberg, D.; Kleinermanns, K. *J. Phys. Chem.* **1998**, *A102*, 4471.
(52) Robertson, E. G.; Hockridge, M. R.; Jelfs, P. D.; Simons, J. P. *J. Phys. Chem.* **2000**, *A104*, 11714.
(53) Robertson, E. G. *Chem. Phys. Lett.* **2000**, *325*, 299.
(54) Robertson, E. G.; Simons, J. P. *Phys. Chem. Chem. Phys.* **2001**, *3*, 1 and references therein.
(55) Carney, J. R.; Hagemeister, F. C.; Zwier, T. S. *J. Chem. Phys.* **1998**, *108*, 3379.
(56) Carney, J. R.; Zwier, T. S. *J. Phys. Chem.* **1999**, *103*, 9943.
(57) Florio, G. M.; Gruenloh, C. J.; Quimpo, R. C.; Zwier, T. S. *J. Chem. Phys.* **2000**, *113*, 11143.
(58) Carney, J. R.; Zwier, T. S. *J. Phys. Chem.* **2000**, *A104*, 8677.
(59) Hagemeister, F. C.; Gruenloh, C. J.; Zwier, T. S. *Chem. Phys.* **1998**, *239*, 83.
(60) Flaud, J. M.; Camy-Peyret, C.; Maillard, J. P. *Mol. Phys.* **1976**, *32*, 499.
(61) Okuzawa, Y.; Fujii, M.; Ito, M. *Chem. Phys. Lett.* **1990**, *171*, 341.
(62) Omi, T.; Shitomi, H.; Sekiya, N.; Takazawa, K.; Fujii, M. *Chem. Phys. Lett.* **1996**, *252*, 287.
(63) Becke, A. D. *Phys. Rev. A*, **1988**, *38*, 3098.
(64) Frisch, M. J.; Trucks, G. W.; Head-Gordon, M.; Gill, P. M. W.; Wong, M. W.; Foresman, J. B.; Johnson, B. G.; Schlegel, H. B.; Robb, M. A.; Replogle, E. S.; Gomperts, R.; Andres, J. L.; Raghavachari, K.; Binkley, J. S.; Gonzalez, C.; Martin, R. L.; Fox, D. J.; Defrees, D. J.; Baker, J.; Stewart, J. J. P.; Pople, J. A. *Gaussian 92*, Revision E.2; Gaussian, Inc.: Pittsburgh, PA, 1992.

(65) Frisch, M. J.; Trucks, G. W.; Schlegel, H. B.; Gill, P. M. W.; Johnson, B. G.; Robb, M. A.; Cheeseman, J. R.; Keith, T.; Petersson, G. A.; Montgomery, J. A.; Raghavachari, K.; Al-Laham, M. A.; Zakrzewski, V. G.; Ortiz, J. V.; Foresman, J. B.; Cioslowski, J.; Stefanov, B. B.; Nanayakkara, A.; Challacombe, M.; Peng, C. Y.; Ayala, P. Y.; Chen, W.; Wong, M. W.; Andres, J. L.; Replogle, E. S.; Gomperts, R.; Martin, R. L.; Fox, D. J.; Binkley, J. S.; Defrees, D. J.; Baker, J.; Stewart, J. P.; Head-Gordon, M.; Gonzalez, C.; Pople, J. A. *Gaussian 94, Revision B.2*; Gaussian, Inc.: Pittsburgh, PA, 1995.

(66) Frisch, M. J.; Trucks, G. W.; Schlegel, H. B.; Scuseria, G. E.; Robb, M. A.; Cheeseman, J. R.; Zakrzewski, V. G.; Montgomery, Jr., J. A.; Stratmann, R. E.; Burant, J. C.; Dapprich, S.; Millam, J. M.; Daniels, A. D.; Kudin, K. N.; Strain, M. C.; Farkas, O.; Tomasi, J.; Barone, V.; Cossi, M.; Cammi, R.; Mennucci, B.; Pomelli, C.; Adamo, C.; Clifford, S.; Ochterski, J.; Petersson, G. A.; Ayala, P. Y.; Cui, Q.; Morokuma, K.; Malick, D. K.; Rabuck, A. D.; Raghavachari, K.; Foresman, J. B.; Cioslowski, J.; Ortiz, J. V.; Stefanov, B. B.; Liu, G.; Liashenko, A.; Piskorz, P.; Komaromi, I.; Gomperts, R.; Martin, R. L.; Fox, D. J.; Keith, T.; Al-Laham, M. A.; Peng, C. Y.; Nanayakkara, A.; Gonzalez, C.; Challacombe, M.; Gill, P. M. W.; Johnson, B.; Chen, W.; Wong, M. W.; Andres, J. L.; Gonzalez, C.; Head-Gordon, M.; Replogle, E. S.; Pople, J. A. *Gaussian 98, Revision A.7*; Gaussian, Inc.: Pittsburgh, PA, 1998.

(67) Cane, E.; Palmieri, P.; Tarronoi, R.; Trombetti, A. *J. Chem. Soc., Faraday Trans.* **1994**, *90*, 3213.

(68) Nakajima, A.; Negishi, Y.; Hasumi, R.; Kaya, K. *Eur. Phys. J.* **1999**, *D9*, 303.

(69) Gordon, M. S. *J. Phys. Chem.* **1996**, *100*, 3974.

(70) Ohashi, K.; Nakai, Y.; Shibata, T.; Nishi, N. *Laser Chem.* **1994**, *14*, 3.

(71) Ohashi, K.; Inokuchi, Y.; Nishi, N. *Chem. Phys. Lett.* **1996**, *263*, 167.